Journal of the Korean Ceramic Society
Vol. 39, No. 10, pp. 907~911, 2002.

Effect of Surface Energy Anisotropy on the Equilibrium Shape of Sapphire Crystal

Jung-Hae Choi†

Center for Microstructure Science of Materials and School of Materials Science and Engineering
College of Engineering, Seoul National University, Seoul 151-742, Korea
(Received September 11, 2002; Accepted September 18, 2002)

ABSTRACT

Using the two-dimensional Wulff plot, the equilibrium shape of a sapphire crystal was investigated as a function of surface energy anisotropy. Depending on the relative values of surface energy for various facet planes, the projected shape of equilibri um sapphire was determined to be rectangle, parallelogram, hexagon or octagon. The results are compared with the experimentally observed shapes of internal cavities of submicron range in sapphire single crystals.

Key words **: *Equilibrium shape, Sapphire, Surface energy anisotropy***

1. Introduction

The Wulff theorem[1-3] predicts that the equilibrium shape of a crystal with the minimum surface energy can be determined by plotting the surface energy values, γ, on the polar diagram (the length of the radius coordinate is taken to be proportional to the γ for the surface perpendicular to the direction of the radius vector). As shown in Fig. 1(a), the inner envelope of the planes, drawn perpendicular to the radius vectors where they cut the imaginary γ-plot (indicated as curved lines) corresponds to the equilibrium shape (shown by the shaded area). Therefore, one of the general features of the equilibrium crystal shape is the presence of facets corresponding to a few cusps in γ-plot. Note from Fig. 1(b) that the planes lying outside the constructed inner shape, such as plane P_i, will not appear in equilibrium even though they correspond to the cusps.

Furthermore, it can be noted from Fig. 1(c) that the presence of plane P_i is dependent on the surface energies of adjacent planes and the interplanar angles, θ. Assuming γ_i is the highest among them, then the anisotropy ratio defined such as either $A_{ij}=\gamma_i/\gamma_j$ and $A_{ik}=\gamma_i/\gamma_k$ is larger than 1. When A_{ij} exceeds A_{ij}^{max} which is defined as $1/\cos\theta_{ij}$, the plane P_i cannot usually appear in equilibrium as shown in Fig. 1(b). In this case, the presence of plane P_i is determined whether the surface energy of another adjacent plane, γ_k, is larger than γ_k^{crit} or not (Fig. 1(c)). Therefore, it is also evident that the crystal shape itself is dependent on the A values between adjacent planes.

†Corresponding author : Jung-Hae Choi
E-mail : choijh@plaza1.snu.ac.kr
Tel : +82-2-880-8862 Fax : +82-2-882-8164

On the other hand, Fig. 2 shows the cavities which have formed "negative" crystals in sapphire.[4] They were obtained by annealing the sapphire containing indentation cracks at 1600°C. As has been described earlier,[4] equilibrium could be reached only for cavities smaller than 100 nm.

The aim of this paper is to predict the equilibrium shape of sapphire crystal as a function of relative surface energies of the experimentally observed equilibrium planes. Recent investigation on sapphire[4] has shown that its equilibrium shape in air is an almost equiaxed and faceted polyhedron bounded by the basal (**C**) {0001}, pyramidal (**P**) {11$\bar{2}$3}, prismatic (**A**) {1$\bar{2}$10}, morphological rhombohedral (**R**) {$\bar{1}$012} and the structural rhombohedral (**S**) {10$\bar{1}$1} planes (The crystallographic notations based on the structural hexagonal cells are used with $c/a=2.730$).[5] These facet planes have also been reported for cavities in sapphire by Kitayama *et al.*[6] Contrary to the theoretical predictions,[7] the prismatic (**M**) {10$\bar{1}$0} planes were not observed to be facet planes.[4,6,8,9] On the other hand, it has been reported[10-19] that the Al_2O_3 grains in silicate liquid are plate-like with well-developed **C** plane. Although the shape was critically dependent on the composition of liquid, **A**, **P**, **R** and **S** were also observed to be the main off-basal facets. From these results, we assumed that the facets in equilibrium sapphire are only **C**, **A**, **P**, **R** and **S** and considered the effect of anisotropy of on the crystal shape.

2. Results and Discussion

When the equilibrium sapphire polyhedron is observed along the zone axes such as <10$\bar{1}$0>, <1$\bar{2}$10> and <10$\bar{1}$1>, the two-dimensional polygons composed of straight line segments will appear and these segments correspond to the edge-on facets. For instance, the equilibrium polyhedron

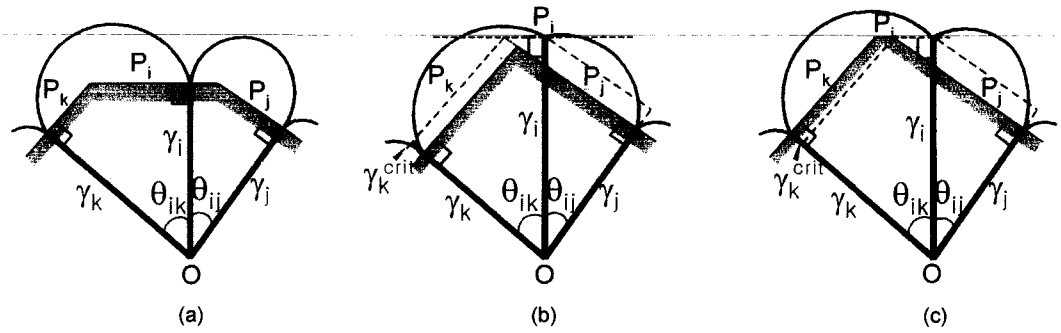

Fig. 1. A part of two-dimensional γ-plot for planes P_i, P_j and P_k where the point O is the center of a crystal : (a) plane P_i will appear when $A_{ij}=\gamma_i/\gamma_j < A_{ij}^{max}$ and $A_{ik}=\gamma_i/\gamma_k < A_{ik}^{max}$: (b) plane P_i will disappear when $A_{ij}=\gamma_i/\gamma_j \geq A_{ij}^{max}$ and $\gamma_k \leq \gamma_k^{crit}$: (c) plane P_i will appear when $A_{ij}=\gamma_i/\gamma_j \geq A_{ij}^{max}$ and $\gamma_k > \gamma_k^{crit}$. The equilibrium crystal shapes are illustrated by shaded areas.

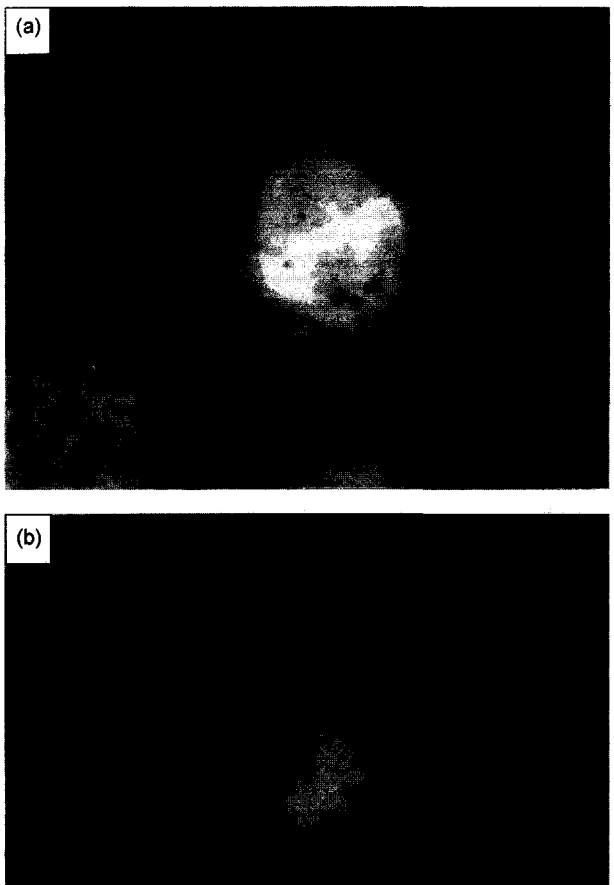

Fig. 2. TEM micrograph of cavities representing the equilibrium crystal shapes in sapphire annealed at 1600°C in air. The zone axis is (a) <1$\bar{2}$10>, (b) <10$\bar{1}$0>, respectively.[4]

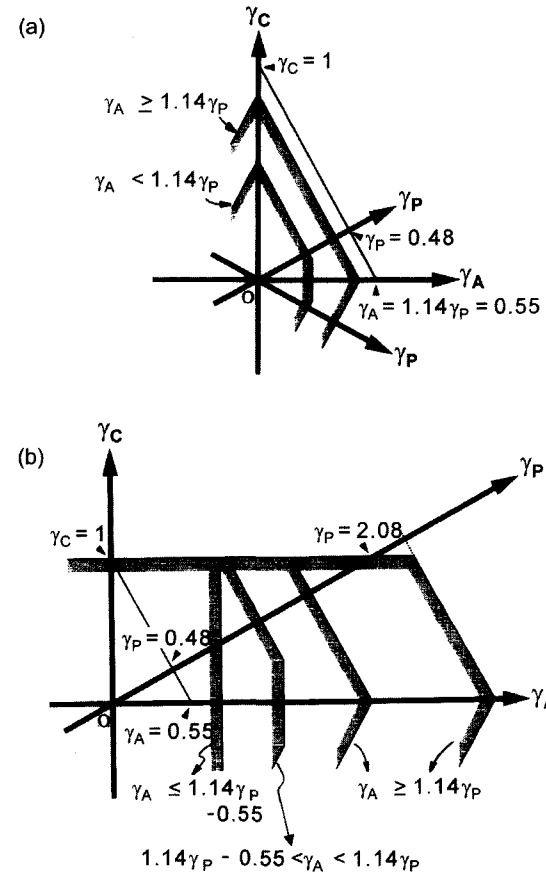

Fig. 3. The two-dimensional γ-plot of the sapphire crystal projected along the <10$\bar{1}$0> zone axis : (a) when $\gamma_P \leq 0.48\gamma_C$: (b) when $\gamma_P > 0.48\gamma_C$. The corresponding equilibrium shapes are illustrated by shaded areas.

projected along the <10$\bar{1}$0> zone axis is a polygon bounded by the **C**, **P** and **A** planes (line segments). The two-dimensional γ-plot and the corresponding crystals composed of these **C**, **P** and **A** planes are illustrated in Fig. 3, where θ_{CP}= 61.2°, θ_{AP}=28.8° and θ_{AC}=90°. The surface energies of **A** and **P** planes are presented by the relative values to that of **C** plane (i.e., γ_C=1 is assumed).

Taking the line perpendicular to the axis of γ_P (**P** plane) which intersects at γ_C=1 (Fig. 3(a)), it can be noted that the **C** plane will not appear in equilibrium if $\gamma_P \leq 0.48$. In this condition, the crystal shape will be determined by γ_A and γ_P. When $\gamma_A \geq (1/\cos\theta_{AP}) \cdot \gamma_P = 1.14\gamma_P$, then γ_A/γ_P becomes greater

than A_{AP}^{max}. As a consequence, the **A** plane will not be present in equilibrium and a diamond-like shape consisting only of **P** facets will appear. When $\gamma_A < 1.14\gamma_P$, on the other hand, the equilibrium shape will be a hexagon composed of **A** and **P** facets. These equilibrium shapes are illustrated by shaded areas in Fig. 3(a).

When $\gamma_P > 0.48$, three different equilibrium shapes depending on γ_A and γ_P will be obtained as shown in Fig. 3(b). If $\gamma_A \geq 1.14\gamma_P$, the hexagon consisting of **C** and **P** facets will appear in equilibrium. When $\gamma_A \leq 1.14\gamma_P - 0.55$, on the other hand, **P** facets will disappear and the rectangle bounded by **C** and **A** planes will be obtained. When γ_A is in the intermediate range of $1.14\gamma_P - 0.55 < \gamma_A < 1.14\gamma_P$, the **A**, **C** and **P** facets will all appear in equilibrium and they will form an octagon in two-dimension. Note also from the figure that the **P** facet can be present eventhough its A_{CP} value is beyond the limit (i.e., $\gamma_P/\gamma_C\, A_{CP}^{max}$=2.08). For this case, the plane adjacent to **P** is crystallographically equivalent one, so it becomes stable even if γ_P exceeds 2.08; the surface normal to **P** lies on its extension (indicated as a dotted line).

In Fig. 4, the equilibrium shapes of sapphire crystal, when they are projected along the <10$\bar{1}$0> zone axis, are summarized as a function of surface energies of **A**, **C** and **P** planes. The x- and y-axes are the normalized surface energies, γ_P/γ_C and γ_A/γ_C, respectively. Although there are five different shapes from rectangle to octagon as already shown in Fig. 3, the shapes without **C** plane, such as diamond-like one consisting only of **P** facets and a hexagon consisting of **A** and **P** facets are hardly expected to appear. Note that the basal **C** plane has been reported to exhibit the lowest surface energy among various planes,[4,10-15] i.e., the γ_A/γ_C, γ_P/γ_C are all greater than 1. In this respect, the dashed region where $\gamma_P/\gamma_C < 1$ or $\gamma_A/\gamma_C < 1$ would not have a real physical meaning.

In the region where $\gamma_P/\gamma_C > 1$ and $\gamma_A/\gamma_C > 1$, the increase of γ_A or γ_P causes the decrease of the area (length in two-dimension) of **A** or **P** facet, respectively. Therefore, the equilibrium shape becomes an elongated plate-like polygon with well-developed **C** plane as illustrated in the figure. In fact, the equilibrium Al_2O_3 facet planes in contact with anorthite liquid observed along the <10$\bar{1}$0> zone axis were reported[10] to be only **C** and **P** planes. For this case, the two dimensional shape of the crystal will be a hexagon as shown in the upper-left region of Fig. 4 with relatively large γ_A. On the other hand, the octagon composed of **C**, **P** and **A** facets is in equilibrium only when the difference between γ_A and γ_P is quite small (indicated by the shaded area).

When the sapphire crystal is projected along the <10$\bar{1}$0>, it can be noted from Fig. 4 that the appearance of three different facet planes, **C**, **P** and **A**, is under very limited conditions. This can be easily explained in terms of relatively small θ_{AP}=28.8°. In other words, A_{AP}^{max} is so small (=1.14) that both **A** and **P** facets can appear only in the very narrow range. As a result, a small change in surface energies of **A** and **P** planes due to segregation may result in the disappearance of either the **P** or **A** plane.

Through the analysis similar to the preceding section, the shape of sapphire crystal projected along the <1$\bar{2}$10> direction has been analyzed and the results are shown in Fig. 5. Note in this case that the **C**, **R** and **S** facets are edge-on and thus the variation of equilibrium shape as a function of their relative surface energies is considered. In Fig. 5, the x- and y-axes are the normalized surface energies, γ_S/γ_C and γ_R/γ_C, respectively. The region where $\gamma_R/\gamma_C < 1$ or $\gamma_S/\gamma_C < 1$ can also be excluded in consideration. Anyhow, when γ_S/γ_C and γ_R/γ_C are smaller than 0.30 and 0.54, respectively, the projected shape will be a diamond-like polygon consisting of **R** and **S** facets. If $\gamma_R \geq 0.89\gamma_S + 0.80$, the parallelogram consisting of **C** and **S** facets will appear in equilibrium. When $\gamma_R \leq 0.89\gamma_S - 0.80$, on the other hand, **R** facet will substitute for **S**. Between the two limits (the shaded area in Fig. 5), the **C**, **R** and **S** facets will all appear and they will form a hexagon. Note that the three different facet planes can appear in a broader range compared to the case of Fig. 4 because A_{RS}^{max} (=1.55) is much larger than A_{AP}^{max}. As a result, the appearance of three

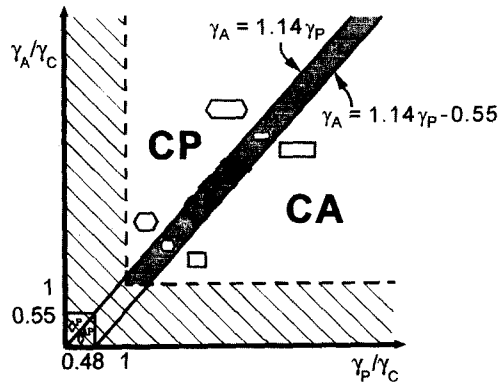

Fig. 4. Variation of two-dimensional equilibrium shape with relative surface energies of **C**, **A** and **P** planes when a crystal is projected along the <10$\bar{1}$0> zone axis.

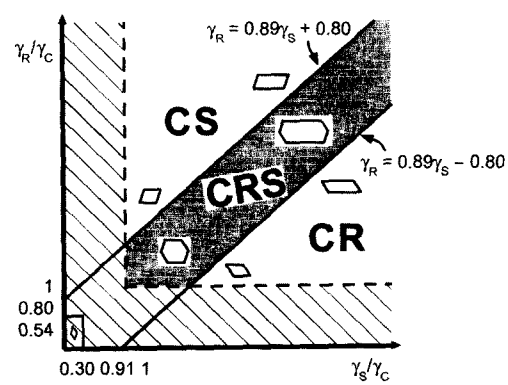

Fig. 5. Variation of two-dimensional equilibrium shape with relative surface energies of **C**, **R** and **S** planes when a crystal is projected along the <1$\bar{2}$10> zone axis.

different facet planes would be much more probable when the crystal is projected along the <1$\bar{2}$10> direction than along the <10$\bar{1}$0>.

In order to determine the three-dimensional shape of sapphire crystal, it is necessary to provide a more complete description including γ_A/γ_C, γ_P/γ_C, γ_R/γ_C and γ_S/γ_C at the same time. In fact, all the concerned facets are edge-on when the crystal is projected along the <10$\bar{1}$1> zone axis : **A**, **R** and two sets of **P** and **S** facets will appear as boundary line segments. Note that A_{RP}^{max}=1.11, A_{PS}^{max}=1.15 and A_{AS}^{max}=1.21 are all fairly small and comparable to A_{AP}^{max} (=1.14). This implies that γ_A, γ_P, γ_R and γ_S should be all similar in order that these four planes are present simultaneously in equilibrium.

On the other hand, the angle between the **C** plane and **P**, **R** and **S** planes are θ_{CP}=61.2°, θ_{CR}=57.6° and θ_{CS}=72.4°, respectively and their A^{max} values are 2.08, 1.87 and 3.31, respectively. For those planes, as already shown in Fig. 4 and Fig. 5, **P**, **R** and **S** can coexist, respectively, with **C** even though their A values (γ_i/γ_C) exceed A_{iC}^{max}. As a consequence, **A**, **P**, **R** and **S** facets can be present simultaneously as the off-basal planes in a **C**-developed plate-like equilibrium crystal as well as in an equiaxed one. Finally, it should be noted that the sharp corners of polygons illustrated in Fig. 4 and Fig. 5 would become truncated and rounded when the adjacent facets which are not edge-on have rather small surface energy. In this case, their segments will appear in the rounded corners with main linear segments resulting from edge-on facets in TEM images as indicated by the arrow in Fig. 2(a).

3. Conclusion

The equilibrium shape of sapphire crystal was analyzed as a function of surface energy anisotropy between **C**, **A**, **P**, **R** and **S** planes. When the crystal is projected along the <10$\bar{1}$0> direction, the hexagon composed of **C** and **P** facets, the rectangle composed of **C** and **A** facets and the octagon composed of **C**, **A** and **P** facets are possible equilibrium shape. For sapphire, the octagon composed of **C**, **A** and **P** facets is observed to be an equilibrium shape, which implies that the difference between γ_A and γ_P is very small. Along the <1$\bar{2}$10> direction, on the other hand, the hexagon composed of **C**, **R** and **S** planes is the probable equilibrium shape. The parallelograms composed of **C** and either **S** or **R** will also appear when either γ_R/γ_C or γ_S/γ_C is relatively large. It is predicted that the equilibrium sapphire crystal composed of **C**, **A**, **P**, **R** and **S** planes is either a basal platelet or an equiaxed polyhedron with similar γ_A, γ_P, γ_R and γ_S.

Acknowledgment

Work is supported by the Creative Research Initiatives of the Korean Ministry of Science and Technology.

REFERENCES

1. G. Wulff, "Zur Frage der Geschwindigkeit des wachstumas und der Aufl sung der Krystallflachen," *Z. Kristallogr.*, **34** 449-530 (1901).
2. C. Herring, "Some Theorems on the Free Energies of Crystal Surfaces," *Phys. Rev.*, **82** [1] 87-93 (1951).
3. J. W. Gibbs, "On the Equilibrium of Heterogeneous Substrates," in *The Scientific Papers of J. W. Gibbs, Vol. I., Thermodynamics,* pp. 54-353 (322), Dover Publications Inc., New York, 1961.
4. J.-H. Choi, D.-Y. Kim, B. J. Hockey, S. M. Wiederhorn, C. A. Handwerker, J. E. Blendell, W. C. Carter and A. R. Roosen, "Equilibrium Shape of Internal Cavities in Sapphire," *J. Am. Ceram. Soc.*, **80** [1] 62-8 (1997).
5. M. L. Kronberg, "Plastic Deformation of Single Crystals of Sapphire : Basal Slip and Twinning," *Acta. Metall.*, **5** [9] 507-24 (1957).
6. M. Kitayama, J. D. Powers, L. Kulinsky and A. M. Glaeser, "Surface and Interface Properties of Alumina via Model Studies of Microdesigned Interfaces," *J. Euro. Ceram. Soc.*, **19** [13-14] 2191-209 (1999).
7. I. Manassidis and M. J. Gillan, "Structure and Energetics of Alumina Structures Calculated from First Principles," *J. Am. Ceram. Soc.*, **77** [2] 335-38 (1994).
8. M. Kitayama and A. M. Glaeser, "The Wulff Shape of Alumina; III, Undoped Alumina," *J. Am. Ceram. Soc.*, **85** [3] 611-22 (2002).
9. J. R. Heffelfinger and C. B. Carter, "Mechanisms of Surface Faceting and Coarsening," *Surf. Sci.*, **389** 188-200 (1997).
10. D.-Y. Kim, S. M. Wiederhorn, B. J. Hockey, C. A. Handwerker and J. E. Blendell, "Stability and Surface Energies of Wetted Grain Boundaries in Aluminum Oxide," *J. Am. Ceram. Soc.*, **77** [2] 444-53 (1994).
11. C. A. Powell-Dogan and A. H. Heuer, "Microstructure of 96% Alumina Ceramics : I, Characterization of the As-Sintered Materials," *J. Am. Ceram. Soc.*, **73** [12] 3670-76 (1990).
12. Y. K. Simpson and C. B. Carter, "Faceting Behavior of Alumina in the Presence of a Glass," *J. Am. Ceram. Soc.*, **73** [8] 2391-98 (1990).
13. H. Song and R. L. Coble, "Morphology of Platelike Abnormal Grains in Liquid-phase-sintering Alumina," *J. Am. Ceram. Soc.*, **73** [7] 2086-90 (1990).
14. Y. Finkelstein, S. M. Wiederhorn, B. J. Hockey, C. A. Handwerker and J. E. Blendell, "Migration of Sapphire Interfaces into Vitreous Bonded Alumina Oxide," pp. 258-79 in Ceramic Transactions, Vol. 7, *Sintering of Advanced Ceramics*. Edited by C. A. Handwerker, J. E. Blendell and W. A. Kaysser, Am. Ceram. Soc., Westerville, OH. 1990.
15. W. A. Kaysser, M. Sprissler, C. A. Handwerker and J. E. Blendell, "Effect of a Liquid Phase on the Morphology of Grain Growth in Alumina," *J. Am. Ceram. Soc.*, **70** [5] 339-43 (1987).
16. S. C. Hansen and D. S. Phillips, "Grain-boundary Microstructures in a Liquid-phase Sintered Alumina (α-Al_2O_3)," *Philos. Mag. A*, **47** 209-34 (1983).
17. D. S. Phillips and Y. R. Shiue, "Grain Boundary Microstructures in Alumina Ceramics," pp. 357-67 in Advances

in Ceramics, Vol. 10, *Structures and Properties of MgO and Al_2O_3 Ceramics*. Ed. by W. D. Kingery, Am. Ceram., Soc., Columbus, OH, 1984.

18. S. C. Hansen and D. S. Phillips, "Grain-boundary Microstructures in a Commercial Alumina Ceramic," pp. 163-70 in Advances in Ceramics, Vol. 6, *Character of Grain Boundaries*, Ed. by M. F. Yan and A. H. Heuer, The Am. Ceram. Soc., Columbus, OH. 1983.
19. K. J. Morrissey and C. B. Carter, "Dislocations in Twin Boundaries in Al_2O_3," pp. 85-95 in Advances in Ceramics, Vol. 6, *Character of Grain Boundaries*, Ed. by M. F. Yan and A. H. Heuer, The Am. Ceram. Soc., Columbus, OH. 1983.